THE JOURNAL OF PHYSICAL CHEMISTRY B

ARTICLE

pubs.acs.org/JPCB

Thermodynamics of the Protonation Equilibria of Two Fragments of N-Terminal β-Hairpin of FPB28 WW Domain

Joanna Makowska,* Dorota Uber, and Lech Chmurzyński

Faculty of Chemistry, University of Gdańsk, Sobieskiego 18, 80-952 Gdańsk, Poland

ABSTRACT: The pK_a values of two peptides derived from *the formin-binding* protein 28 WW domain [Ac-Lys-Thr-Ala-Asp-Gly-Lys-Thr-NH_2 (D7), Ac-Tyr-Lys-Thr-Ala-Asp-Gly-Lys-Thr-Tyr-NH_2 (D9)] were determined by potentiometric titration in the temperature range from 25 to 60 °C, and their heat capacities were determined, by differential scanning calorimetry, in the temperature range from 10 to 90 °C. For both peptides, heat capacity has a maximum at $t \approx 50$ °C, with height about 0.1 kcal/(mol × deg), suggesting that a modest unfolding transition occurs. The first two pK_a's are low at temperatures below 50 °C, suggesting that the two lysine residues are close to each other and the peptides have bent shapes at lower temperatures; this effect is greater for D7 compared with D9. With increasing temperature beyond 50 °C (i.e., that of the thermodynamic unfolding transition), pK_{a1} and pK_{a2} increase rapidly for D9, whereas their temperature variation is less significant for D7. This observation, and the fact that the enthalpies and entropies of the dissociation of the two first protons (determined from the temperature dependence of the respective pK_a's) decrease significantly near the transition temperature, suggest that the peptide undergoes a transition from a bent to an amorphous shape and that the presence of charged lysine residues stabilizes the folded state.

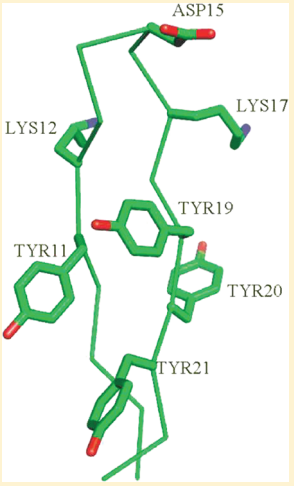

1. INTRODUCTION

Some short peptide fragments excised from proteins can fold in aqueous solution into conformations with shape similar to that assumed in the parent protein even though they lack fine details such as hydrogen-bonding network.[1] Thus, these fragments may play an important role as nucleation centers in initiating protein folding[2−4] through local interactions.

The literature is rich in reports from the studies of the kinetics and thermodynamics of the formation of α-helical structure in peptides.[5−12] For example, a lot of studies showed that the replacement of interior helical residues with alanine residues has considerable influence on the stability of α-helical peptides. This led to the successful design of isolated, monomeric helical peptides in aqueous solution, containing several salt bridges and a high alanine content[13] or a simple sequence with a high alanine content with several lysine residues to increase solubility.[14] However, much less is known about the formation of β-type structures, which is indispensable to understand better the protein folding process.

Single amino-acid substitutions that reverse or remove the charges on solvent-exposed side chains have been shown to increase protein stability without altering the structure in some cases.[15,16] Similarly, the pH and salt dependence of β-hairpin formation in a number of model systems suggest that long- and short-range electrostatic interactions across β-strands can also contribute to stability.[17−20] Muñoz and co-workers[21] suggested a mechanism of creating turns in β-hairpins through "buttoning up" hydrogen bonds and hydrophobic interactions. Karplus and co-workers[22] emphasized the dominant role of hydrophobic collapse of this part of the sequence. On the basis of our studies of the folding of the peptides excised from the C-terminal β-hairpin of the immunoglobulin binding protein (IGG1),[23−25] in our recent work[26] we concluded that the initial formation of chain reversals results from many interactions, in which the interplay between turn and hydrophobic-contact formation are of key importance. Additionally, from our studies of alanine-based peptides,[27,28] we concluded that the presence of charged groups (like or oppositely charged) on both ends of a short chain fragment might be another factor contributing to the formation of chain reversals because the charged groups could screen the nonpolar core from the solvent. However, these studies concerned model systems not directly related to real proteins. Therefore, in the present study we investigated the N-terminal β-hairpin from the tryptophan-rich domain of the formin-binding protein 28 (FBP28 WW domain). Formation of the C-terminal β-hairpin has been shown to be the first stage of the folding of FBP28 WW domain.[29,30] The structure of this β-hairpin is shown in Figure 1. This hairpin contains two lysine residues (Lys12 and Lys17) at the ends, which are close to each other in the experimental 1E0L structure[31] of the protein. The β-hairpin is apparently stabilized by a hydrophobic contact between the side chains of Tyr11 and Tyr19. We studied the following two peptides: WW(11−19) (9 residues, hereafter referred to as D9) and WW(12−18) (7 residues, hereafter referred to as D7). Detailed

Received: October 13, 2011
Revised: November 29, 2011
Published: November 29, 2011

dx.doi.org/10.1021/jp209844v | J. Phys. Chem. B 2012, 116, 653–659

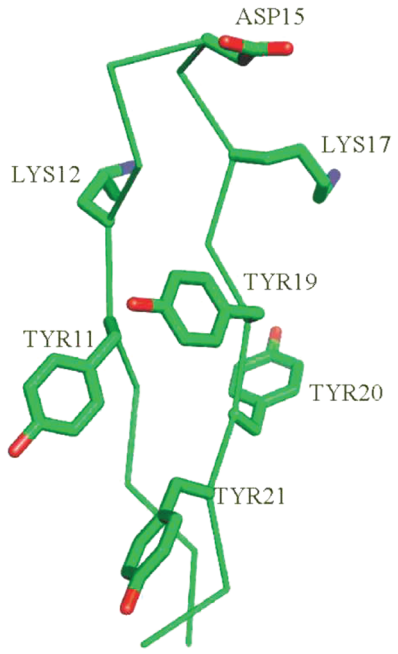

Figure 1. Structure of the N-terminal β-hairpin from FBP28 WW domain. The backbone is shown as an α-carbon trace, and the ionizable side chains (Tyr11, Lys12, Asp15, Lys17, Tyr19) are shown in stick representation.

amino-acid sequences of these peptides are Ac-Tyr-Lys-Thr-Ala-Asp-Gly-Lys-Thr-Tyr-NH_2 and Ac- Lys-Thr-Ala-Asp-Gly-Lys-Thr- NH_2, respectively. The second peptide cannot form the Tyr...Tyr hydrophobic contact that apparently stabilizes the N-terminal β-hairpin in the parent protein.

The determination of pK_a values can provide some information regarding the neighborhood of an ionizable group.[32−34] In particular, in our earlier studies of the $(Dab)_2$-$(Ala)_7$-$(Orn)_2$ peptide (usually referred to as XAO),[35] we found that pK_{a1} is abnormally low (2.72, compared to the value of 10.87 for ethylamine, which can be considered a model of the side chain of diaminobutyric acid), which suggests that the charged groups are close to each other, implying a bent shape. Our NMR studies[36] and the SAXS studies by Zagrovic et al.[37] demonstrated that, as a matter of fact, this peptide does have a bent shape. Similar results were obtained from our potentiometric[27] and NMR[28] studies of three other alanine-based peptides. Therefore, in this study, we determined the pK_a values of D7 and D9 in water. Moreover, the pK_a values were determined in a temperature range from 25 to 60 °C to assess how their variation correlates with the thermodynamic transition point, which we additionally studied by means of differential-scanning calorimetry, and to determine thermodynamic functions (entropy and enthalpy) change upon deprotonation.

2. EXPERIMENTAL METHODS

2.1. Peptide Synthesis. The peptides Ac-Lys-Thr-Ala-Asp-Gly-Lys-Thr-NH_2 (D7) and Ac-Tyr-Lys-Thr-Ala-Asp-Gly-Lys-Thr-Tyr-NH_2 (D9) were synthesized by standard solid-phase Fmoc-amino acid chemistry with a Milipore synthesizer. Both resins Tentagel R RAM (1 g, capacity 0.19 mmol/g) were treated with piperidine (20%) in DMF, and all amino acids were coupled using DIPCI/HOBt methodology. The coupling reaction time was 2 h. Piperidine (20%) in DMF was used to remove the Fmoc group at all steps. After deprotection of the last Fmoc *N*-terminal group, each of the resins was washed with methanol and dried in vacuo. Then the resins were treated with 1 M 1-acetylimidazole in DMF at room temperature for 2 h to attach the acetyl group to the N-terminal part of the peptide. In the final step, the resins were treated with a TFA/water/phenol/triisopropylsilane (8.8/0.5/0.5/0.2) mixture (10 mL per gram of resin) at room temperature for 2 h to remove the peptide from the resin. Each of the resins was separated from the mother liquid; the excess of solvent was then evaporated to a volume of 2 mL, and the residue was precipitated with diethyl ether. The crude peptides were purified by reversed-phase HPLC using a Supelcosil SPLC-ABZ C_{18} semipreparative column (10 × 250 mm, 5 μm) with 4 mL/min elution and a 120 min isocratic mixture of 0.5% CH_3CN, in TFA to adjust the pH approximately to 2.0. To identify fractions containing the pure peptides, HPLC was run first with a small amount of the crude peptide and the absorbance at 222 nm was measured for each fraction. A plot of absorbance vs retention time was constructed and the interval of the retention time to separate the pure peptide was estimated as that corresponding to the large peak in the plot. Subsequently, a semipreparative HPLC run was carried out and the fractions containing the pure peptide were collected and lyophilized. The purity of each peptide was confirmed by analytical HPLC and MALDI-TOF analysis (Table 1).

2.2. Differential Scanning Calorimetry (DSC). Calorimetric measurements were made with a VP-DSC microcalorimeter (MicroCal) at a scanning rate of 90 °C/1 h. Scans were obtained at protein concentrations of $c \sim 0.181$ mM and $c \sim 0.165$ mM for D7 and D9, respectively. The cell volume was 0.5 mL. All scans were run in water in the range of temperature 5−90 °C. The pH of the water used to dissolve the samples was ∼4.6. After the dissolution process, the values of pH for samples of peptides were 3.5 and 3.2 for D7 and D9, respectively.

The reversibility of the transition was checked by cooling and reheating the same sample. These measurements were recorded three times. Results from DSC measurements were analyzed with the Origin 7.0 software from MicroCal using the routines of the software provided with the instrument.[38]

2.3. Potentiometric Titration. All measurements for both D7 and D9 peptides were carried out in an EMF cell containing a microelectrode at temperatures t = 25, 30, 40, 50, and 60 °C. The potentiometric-microtitration unit was equipped with a computer-aided microtitrator system and a millivoltmeter with an acuracy of 0.01 mV. The titrant was added dropwise using a 1 cm^3 HAMILTON syringe with an accuracy of 0.01 cm^3. For each titration, a stock solution of the peptide was prepared at a concentration of approximately 0.001 M; 3 cm^3 of this solution was added to the titration vessel. The titrant contained 0.018 M sodium hydroxide in water.

Before running a series of measurements, the electrode was calibrated for each temperature as follows: 3 cm^3 of NaH_2PO_4 in water solution at a concentration of c = 0.001 M was titrated with aqueous sodium hydroxide at a concentration of approximately 0.01 M. For each titration curve, the parameters $E°$ and S of the electrode equation (eq 1) were obtained by fitting the model of three stepwise acid−base equilibria, given the literature pK_a values of H_3PO_4, $H_2PO_4^-$, and HPO_4^{2-} at each respective temperature (Table 2[39−43]), by using the program STOICHIO.[44,45] The values of $E°$ and S are shown in Table 3.

$$E = E° - S\,\mathrm{pH} \quad (1)$$

dx.doi.org/10.1021/jp209844v |J. Phys. Chem. B 2012, 116, 653–659

Table 1. Types of Resins Used in Peptide Synthesis, Form of Peptide (Free or Block N- and C-Termini), and the Molecular Mass for Each of the Synthesized Peptides

				molecular mass (g/mol)	
peptide	resin used to synthesis	N-terminus	C-terminus	experimental	theoretical
D7	TentaGel R RAM (1 g, capacity 0.19 mmol/g)	acetyl	amide	718.525	718.397
D9	TentaGel R RAM (1 g, capacity 0.19 mmol/g)	acetyl	amide	1044.624	1044.524

Table 2. Literature pK_a Values of HPO_4^{2-}, $H_2PO_4^-$, and H_3PO_4 and at Each Respective Temperature

	temp (°C)				
species	25	30	40	50	60
HPO_4^{2-}	12.325[a]	12.18[b]	11.83[b]	11.7[e]	11.53[e]
$H_2PO_4^-$	7.207[a]	7.197[c]	7.189[c]	7.191[c]	7.196[e]
H_3PO_4	2.161[a]	2.171[d]	2.185[c]	2.26[c]	2.338[d]

[a] Reference 39. [b] Reference 40. [c] Reference 41. [d] Reference 42. [e] Reference 43.

Table 3. Vlues of Intercept ($E°$) and Slope (S) of the Electrode Equation (eq 1; Standard Deviations in Parentheses) and Standard Deviation of Electromotive Force (σ_{EMF}) and Titrant Volume (σ_V) Corresponding to Fitting Electrode Equation to the Titration Data of NaH_2PO_4 with the Program STOICHIO

	25 °C	30 °C	40 °C	50 °C	60 °C
$E°$ S (mV)	394.8 (1.3)	387.4 (2.4)	351.0 (9.7)	352.4 (9.7)	474.2 (4.3)
	57.28 (0.13)	55.97 (0.22)	52.94 (0.92)	54.44 (0.95)	66.65 (0.45)
σ_{EMF} (mV)	1.34	2.44	3.66	3.72	3.79
σ_V (cm^3)	0.0006	0.0007	0.0009	0.0008	0.0004

2.4. Fitting Models of Chemical Equilibria to Titration Curves. Models of acid−base equilibria were fitted to the resulting titration curves by using the program STOICHIO,[44,45] which is based on a nonlinear confluence analysis. This program can treat any model of chemical equilibria and takes into account all possible sources of experimental error (the error in EMF, titrant and titrated solution volume, reagent impurities, etc.). Briefly, the sum of squares to be minimized is expressed by eq 2 (see ref 45 for more details).

$$\Phi = \frac{1}{\sigma_V{}^2}\sum_i (V_i^{exp} - V_i^{calc})^2 + \frac{1}{\sigma_{EMF}{}^2}\sum (EMF_i^{exp} - EMF_i^{calc})^2 + \sum_j \frac{1}{\sigma_{x_j}{}^2}(x_j^{exp} - x_j^{calc})^2 \quad (2)$$

where V denoted titrant volume, σ_V and σ_{EMF} denote the standard deviation of titrant volume and electromotive force, respectively, x_j is a quantity known from other experiments (the $E°$ and S parameters of electrode characteristics, total concentrations of titrant and titrand components, equilibrium constants known from other measurements such as, e.g., the ionic product of water, and σ_{x_j} denotes the standard deviation of parameter x_j. The variables of the minimized sum of squares, Φ, are the equilibrium constants, as well as V^{calc} and x^{calc}. The equilibrium constants to be determined are unrestrained, whereas the variation of other parameters (titrant volumes, etc.) from the measured values is restrained by "force constants" proportional to the inverse of their standard deviations. The superscripts "exp" and "calc" denote the measured and calculated quantities, respectively. All σ's that appear in eq 2 are a priori values, estimated on the basis of the precision of measurements and not a posteriori values calculated after minimization of Φ.[45]

Table 4. pK_a Values (Standard Deviations in Parentheses) for the D7 Peptide in Water at t = 25, 30, 40, 50, and 60 °C Obtained by Fitting the Equilibrium Model of Three-Stage Dissociation to Potentiometric-Titration Data

	25 °C	30 °C	40 °C	50 °C	60 °C
pK_{a1}	3.75 (0.13)	4.89 (0.09)	4.49 (0.08)	2.91 (0.35)	3.97 (0.10)
pK_{a2}	6.62 (0.11)	8.02 (0.06)	8.03 (0.04)	6.47 (0.08)	6.76 (0.07)
pK_{a3}	8.66 (0.16)	9.33 (0.07)	9.64 (0.04)	9.98 (0.08)	9.36 (0.10)
pK_w[a]	14.0 (0.04)	13.84 (0.04)	13.80 (0.02)	13.25 (0.03)	12.96 (0.03)
σ_{EMF}[b]	7.42	3.45	2.71	4.38	3.17
σ_V[c]	0.00015	0.0004	0.0008	0.0011	0.0005

[a] The ionic product of water. [b] Standard deviation of electromotive force. [c] Standard deviation of titrant volume.

On the basis of the accuracy of the measurements, we adopted a standard deviation of σ_{EMF} = 2 mV and σ_V = 0.001 cm^3. We also assigned an a priori relative standard deviation of 1% to the content of protons in fully protonated peptide (σ_{H^+}), because the purification procedure can potentially leave traces of trifluoroacetic acid. Technically, the relative content of protons could vary within $\pm 3\sigma_{H^+}$ during the optimization procedure. The D7 peptide was treated as trifunctional acid (two types of groups) because of three charged groups present in the sequence, and three pK_a values were considered; D9 was treated as a pentafunctional acid (two types of groups), and five pK_a values were considered as parameters to be determined. The ionic product of water (pK_{aw}) was also treated as an adjustable parameter, restraining its literature value at the respective temperature.[46] The standard deviation of pK_{aw} as assumed 0.01 logarithmic unit.

3. RESULTS AND DISCUSSION

The pK_a values of D7 and D9, together with their standard deviations, are summarized in Tables 4 and 5, respectively. On the basis of the magnitude, pK_{a1} of D7 can be assigned to Asp15, and pK_{a2} and pK_{a3} can be assigned to the two lysine residues. For D9, pK_{a1} can be assigned to Asp15, pK_{a2} and pK_{a3} can correspond to either of the two lysine residues, and pK_{a4} and pK_{a5}

Table 5. pK_a Values (Standard Deviations in Parentheses) for the D9 Peptide in Water at t = 25, 30, 40, 50, and 60 °C Obtained by Fitting the Equilibrium Model of Five-Stage Dissociation to Potentiometric-Titration Data

	25 °C	30 °C	40 °C	50 °C	60 °C
pK_{a1}	3.55 (0.09)	3.76 (0.19)	3.41 (0.22)	2.55 (0.38)	4.67 (0.06)
pK_{a2}	3.94 (0.05)	4.49 (0.22)	4.16 (0.25)	3.59 (0.07)	7.44 (0.05)
pK_{a3}	7.46 (0.05)	7.43 (0.09)	7.01 (0.09)	6.64 (0.05)	9.34 (0.10)
pK_{a4}	9.81 (0.05)	9.40 (0.08)	9.71 (0.09)	8.96 (0.04)	9.64 (0.40)
pK_{a5}	10.70 (0.08)	10.34 (0.18)	10.31 (0.19)	10.57 (0.19)	10.22 (0.21)
pK_w [a]	13.93 (0.03)	13.87 (0.02)	13.77 (0.02)	13.26 (0.01)	12.99 (0.01)
σ_{EMF} [b]	0.48	1.7	0.41	0.418	0.81
σ_V [c]	0.0038	0.009	0.0066	0.0054	0.006

[a] The ionic product of water. [b] Standard deviation of electromotive force. [c] Standard deviation of titrant volume.

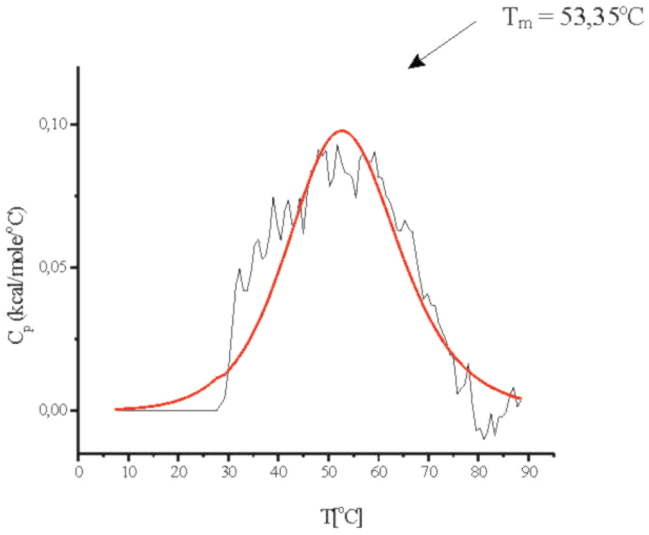

Figure 2. Heat-capacity curve of the D7 peptide determined by DSC (black line) and the fit to the two-state model (red line).

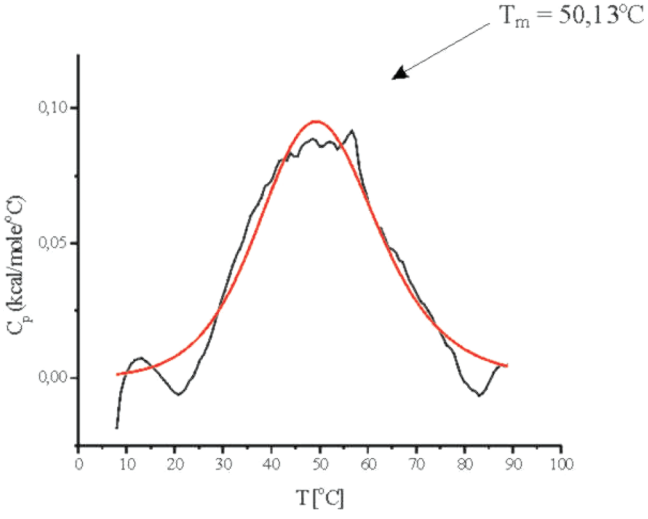

Figure 3. Heat-capacity curve of the D9 peptide determined by DSC (black line) and the fit to the two-state model (red line).

can be assigned to either of the two tyrosine residues. On the basis of our earlier simulation studies of the coupling between the conformation and acid−base equilibria,[35] it can be noted that each of pK_{a2} and pK_{a3} (for D7 and D9), as well as pK_{a4} and pK_{a5} (for D9), as a value averaged over conformations, has contributions from either lysine (pK_{a2} and pK_{a3}) or tyrosine (pK_{a4} and pK_{a5}) residue.

It can be seen that, for both peptides at room temperature (t = 25 °C), pK_{a1} is lower than that of acetic acid (4.76[47]) and pK_{a2} and pK_{a3} are significantly lower than those of *n*-butylamine (10.5[27]), which can be considered a reference compound for the side chain of lysine. This observation can be explained in terms of the influence of positively charged side chains of lysine residue exerting electrostatic field on the aspartic acid side chain and that of the positively charged side chain of the *first* lysine side chain which exerts positive electrostatic field on the second lysine side chain. This effect was observed in our earlier study of alanine-based peptides.[27,35] The value of pK_{a3} (corresponding to the second lysine side chain) is also decreased with respect of that of the reference compound, albeit to a much lesser extent. It seems reasonable that the pK_a's are shifted down because the neighboring side chains are positively charged. The pK_a of the last lysine (in both D7 and D9) is decreased probably because of the proximity of polar peptide groups that act as a basic solvent (for example, the pK_a values determined in formamide are lower than those determined in water[48]).

For D9, there is a very significant increase in pK_{a2} and pK_{a3} (that correspond to lysine side chains) from t = 50 °C to t = 60 °C. This increase clearly exceeds the 99% confidence level (three times the sum of standard deviations). It can, therefore, be concluded that D9 undergoes an unfolding transition in this temperature region. For D7, pK_{a2} also increases from t = 50 °C to t = 60 °C, though not so significantly. It should be noted that the pK_a values of isolated amines decrease with temperature.[49]

Inspection of the heat-capacity curves of D7 and D9 (Figures 2 and 3) indicates that heat-capacity peaks occur at $t \approx$ 50 °C. The positions of the peaks obtained by fitting a two-state model to the heat-capacity curves are $t \approx$ 53.3 °C and $t \approx$ 50.1 °C, respectively; however, the actual maxima occur at $t \approx$ 50 °C for both peptides. For D9 the peak is sharper although it has a low height [about 0.1 kcal/(mol × K)] in both cases. The broad shape of the DSC curves for D7 and D9 peptides suggest the folding−unfolding transition occurs for these two peptides is not sharp and they occur as a mixture of interconverting conformations in a dynamic equilibrium. The noise in the data is caused by low height of the peaks relative to measurement accuracy, which is about 0.01 kcal/(mol × K).

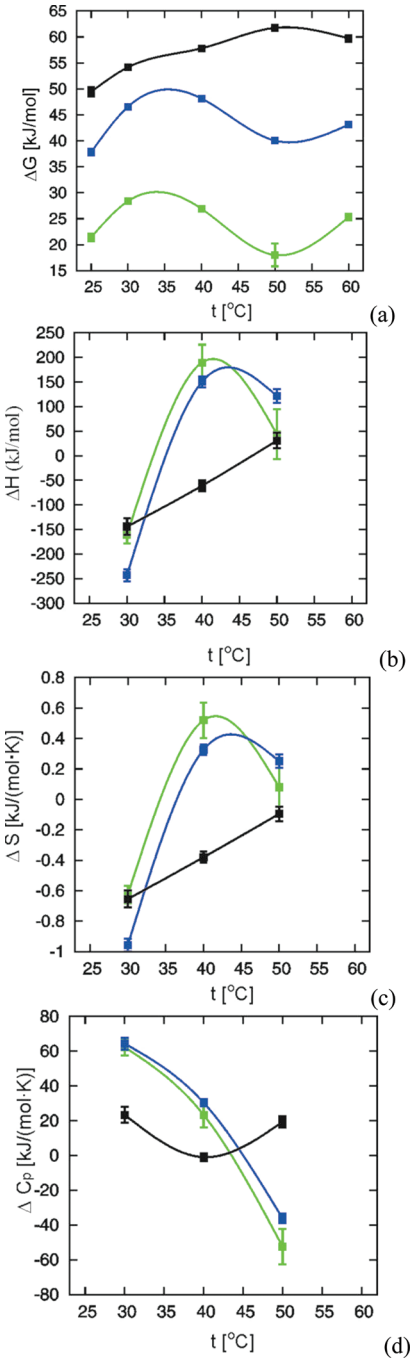

Figure 4. Dependence of the change of (a) Gibbs free energy (ΔG), (b) enthalpy (ΔH), (c) entropy (ΔS), and (d) specific heat (ΔC_p) of deprotonation of consecutive ionizable amino-acid side chains of the D7 peptide in water. The values were calculated on the basis of the pK_a values of D7 collected in Table 3. Vertical lines are error bars, points are experimental points, and lines are cubic-spline interpolation lines between the experimental points. Green, blue, and black lines and symbols correspond to the first, second, and third stage of proton dissociation, respectively.

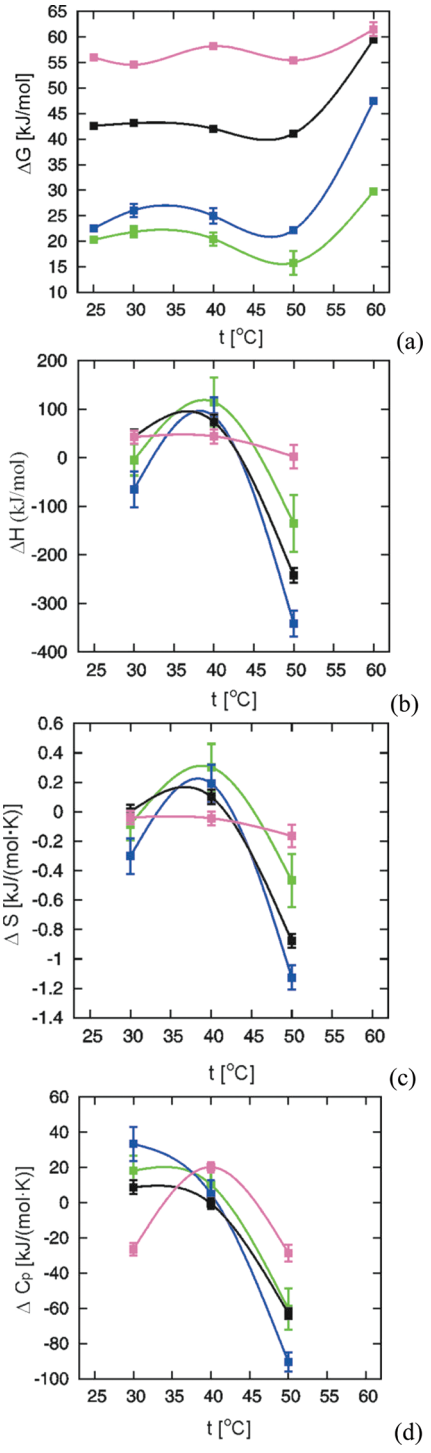

Figure 5. Dependence of the change of (a) Gibbs free energy (ΔG), (b) enthalpy (ΔH), (c) entropy (ΔS), and (d) specific heat (ΔC_p) of deprotonation consecutive ionizable amino-acid side chains of the D9 peptide in water. Vertical lines are error bars, points are experimental points, and lines are cubic-spline interpolation lines between the experimental points. Green, blue, black, purple, and red lines and symbols correspond to the first, second, third, fourth, and fifth stage of proton dissociation, respectively.

It can also be noted that the DSC curves obtained for D7 and D9 exhibit no significantly negative peaks, which demonstrates that the two peptides do not aggregate under the experimental conditions.

To have a better insight into the thermodynamics of the consecutive acid−base equilibria of D7 and D9, we calculated the changes of Gibbs free energy (ΔG), enthalpy (ΔH), entropy (ΔS), and heat capacity (ΔC_p) from the temperature dependence of pK_a values. We used the following

dx.doi.org/10.1021/jp209844v |J. Phys. Chem. B 2012, 116, 653–659

relationships:

$$\Delta G^\circ = \ln 10 \times RT \times \mathrm{p}K_a \quad (3)$$

$$\Delta S^\circ = -\frac{\partial \Delta G^\circ}{\partial T} \quad (4)$$

$$\Delta H^\circ = \Delta G^\circ + T\Delta S^\circ \quad (5)$$

$$\Delta C_p^\circ = -T\frac{\partial^2 \Delta G^\circ}{\partial T^2} \quad (6)$$

The first derivative and second derivatives of ΔG° were estimated from divided differences (symmetrized for the first derivative). The plots of the quantities given by eqs 3−6 are for D7 and D9 are shown in Figures 4a−d and 5a−d, respectively. Therefore, the first and the last points are omitted from the graphs of the thermodynamic quantities except for ΔG°.

As shown, for both peptides, the change of entropy (ΔS°) and enthalpy (ΔH°) corresponding to the first two stages of dissociation initially increases with temperature and then decreases from t = 50 °C to t = 60 °C even to negative values for D9. The changes of heat capacity corresponding to the stepwise dissociation of the two protons (ΔC_p°) behave likewise for the second dissociation step of D9 and decrease monotonically for the remaining instances. These changes are much more pronounced for D9 than for D7. Thus the changes occur in the region of thermodynamic folding transition corresponding to the region of the maxima of the corresponding heat-capacity curves (Figures 3 and 4).

The increase of enthalpy and entropy upon proton dissociation before the transition midpoint means that the protons essentially dissociate from an established ensemble of peptide conformations. This process is endothermic and involves the increase of entropy because of ordering water structure upon proton release to water. The drop of enthalpy, until the point that proton release becomes an exothermic process for D9, and heat capacity upon proton release near the folding-transition point indicate that the folded peptide becomes less favorable energetically upon deprotonation and the folding transition becomes less sharp. Exothermic effects of proton dissociation were also observed for unblocked dipeptides.[47,50] It can, therefore, be concluded that the presence of two charged lysine residues stabilizes the folded state. The decrease of entropy close to transition midpoint indicates that the folded state becomes less ordered relative to the unfolded state upon proton release, this observation also indicates that the presence of charged residues contributes to the stability of the folded ensemble. Also, the fact that the changes of the thermodynamic functions upon the release of the third proton in D7 and that of the last two protons in D9 near the folding-transition temperature are less pronounced than those corresponding to the first two (for D7) or three (D9) stages of proton release indicates that the structures of D7 and D9 might be largely melted after the release of the first two or the first three protons, respectively, thus confirming the stabilizing role of the charged lysine residue(s). The fact that the heat-capacity peak is sharper and changes of ΔG°, ΔH°, ΔS°, and ΔC_p° upon the release of the first two protons are more pronounced for D9 than for D7 can be explained in terms of the presence of two tyrosine side chains at chain ends in D9, which form a hydrophobic contact, additionally stabilizing the structure.

4. CONCLUSIONS

In this work we determined the pK_a values corresponding to subsequent stages of proton release and heat-capacity curves in water for two variants of the sequence corresponding to the N-terminal β-hairpin of the FBP28 WW domain that contain two lysine side chains that flank the β-hairpin structure in the experimental 1E0L structure of the protein,[31] in the range of temperatures from t = 25 °C to t = 60 °C. The sequences of these variants were Ac-Lys-Thr-Ala-Asp-Gly-Lys-Thr-NH_2 (D7; three dissociable protons) and Ac-Tyr-Lys-Thr-Ala-Asp-Gly-Lys-Thr-Tyr-NH_2 (D9; five dissociable protons), respectively. For both peptides, we observed a heat-capacity peak at $t \approx$ 50 °C, which suggest that they are somehow folded at lower temperatures (Figure 2 and 3). The peak is sharper for D9, probably because a pair of tyrosine residues, which form a hydrophobic contact in the experimental structure of the whole protein (Figure 1) can also act so in the D9 peptide. Low values of the first two pK_a's indicate that the ionizable side chains perceive the electrostatic field of the positively charged lysine residue(s), thus suggesting a relatively compact chain-reversal structure. However, this conclusion must be assessed by carrying out structural studies that are now underway in our laboratory.

On the basis of the temperature dependence of the pK_a values, we computed the change of standard Gibbs free energy, enthalpy, entropy, and heat capacity as functions of temperature. We found that the standard Gibbs free energy increases while the standard enthalpy, entropy, and heat capacity decrease close to the thermodynamic unfolding-transition temperature upon the release of the first and the second proton for D7 and that of the first three protons for D9, respectively, indicating that deprotonation destabilizes the folded state.

The results of this study, along with those of our previous work[27,28,36] support the hypothesis that the presence of like-charged residues at the ends of a chain reversal can stabilize its structure. It should be noted that, even though this hypothesis might sound counterintuitive, it is supported by the fact that polylysine chains form α-helical structures at low pH;[51] in these structures, lysine side chains point outside to shield the backbone from solvent.

AUTHOR INFORMATION

Corresponding Author

*E-mail: royek@chem.univ.gda.pl. Phone: +48 58 523 5427. Fax: +48 58 523 5472.

ACKNOWLEDGMENT

This research was conducted by using the resources of the Informatics Center of the Metropolitan Academic Network (IC MAN) in Gdańsk. The publication is financed by the European Social Fund as a part of the project "Educators for the elite - integrated training program for Ph.D. students, post-docs, and professors as academic teachers at the University of Gdańsk" within the framework of the Human Capital Operational Programme, Action 4.1.1, Improving the quality of educational offer of tertiary education institutions. This publication reflects the views of only the authors, and the funder cannot be held responsible for any use which may be made of the information contained therein. This work is supported by grants for Young Scientists 2011 from the University of Gdańsk (JM no. 538-8232-0494-1) of DS/8232-4-0088-1 and from the National Science Centre (UMO-2011/01/D/ST4/04497).

REFERENCES

(1) Searle, M. S.; Williams, D. H.; Packman, L. C. *Nat. Struct. Biol.* **1995**, *2*, 999–1006.
(2) Dill, K. A. *Biochemistry* **1990**, *29*, 7133–7155.
(3) Kim, P. S.; Baldwin, R. L. *Annu. Rev. Biochem.* **1990**, *59*, 631–660.
(4) Karplus, M.; Weaver, D. L. *Protein Sci.* **1994**, *3*, 650–668.
(5) Brown, J. E.; Klee, W. A. *Biochemistry* **1971**, *10*, 470–476.
(6) Silverman, D. N.; Kotelchuck, D.; Taylor, G. T.; Scheraga, H. A. *Arch. Biochem. Biophys.* **1972**, *150*, 757–766.
(7) Jimnez, M. A.; Herranz, J.; Nieto, J. L.; Rico, M.; Santoro, J. *FEBS Lett.* **1987**, *221*, 320–324.
(8) Jimnez, M. A.; Rico, M.; Herranz, J.; Santoro, J.; Nieto, J. L. *Eur. J. Biochem.* **1988**, *175*, 101–109.
(9) Dyson, H. J.; Merutka., G.; Waltho, J. P.; Lerner, R. A.; Wright, P. E. *J. Mol. Biol.* **1992**, *226*, 795–817.
(10) Kuroda, Y. *Biochemistry* **1993**, *32*, 1219–1224.
(11) Munoz, V.; Serrano, L.; Jimnez, M. A.; Rico, M. *J. Mol. Biol.* **1995**, *4*, 648–669.
(12) Blanco, F. J.; Serrano, L. *Eur. J. Biochem.* **1995**, *230*, 634–649.
(13) Park, S. H.; Shalongo, W.; Stellwagen, E. *Biochemistry* **1993**, *32*, 7048–7053.
(14) Marqusee, S.; Robbins, V. H.; Baldwin, R. L. *Proc. Natl. Acad. Sci. U. S. A.* **1989**, *86*, 5286–5290.
(15) Grimsley, G. R.; Shaw, K. L.; Fee, L. R.; Alston, R. W.; Huyghues-Despointes, B. M. P.; Thurlkill, R. L.; Scholtz, J. M.; Pace, C. N. *Protein Sci.* **1999**, *8*, 1843–1849.
(16) Perl, D.; Mueller, U.; Heinemann, U.; Schmid, F. X. *Nat. Struct. Biol.* **2000**, *7*, 380–383.
(17) Huyghues-Despointes, B. M.; Qu, X.; Tsai, J.; Scholtz, J. M. *Proteins* **2006**, *63*, 1005–1017.
(18) de Alba, E.; Blanco, F. J; Jimenez, M. A; Rico, M.; Nieto, J. L. *Eur. J. Biochem.* **1995**, *233*, 283–292.
(19) Ramirez Alvarado, M.; Blanco, F. J.; Serrano, L. *Protein Sci.* **2001**, *10*, 1381–1392.
(20) Olsen, K. A.; Fesinmeyer, R. M; Stewart, J. M.; Andersen, N. H. *Proc. Natl. Acad. Sci. U. S. A.* **2005**, *102*, 15483–15487.
(21) Muñoz, V.; Henry, E. R.; Hofrichter, J.; Eaton, W. A. *Proc. Natl. Acad. Sci. U. S. A.* **1998**, *110*, 5872–5879.
(22) Dinner, A. R.; Lazaridis, T.; Karplus, M. *Proc. Natl. Acad. Sci. U. S. A.* **1999**, *96*, 9068–9073.
(23) Skwierawska, A.; Makowska, J.; Ołdziej, S.; Liwo, A.; Scheraga, H. A. *Proteins: Struct. Funct. Bioinf.* **2009**, *75*, 931–953.
(24) Skwierawska, A.; Żmudzińska, W.; Ołdziej, S.; Liwo, A.; Scheraga, H. A. *Proteins: Struct. Funct. Bioinf.* **2009**, *76*, 637–654.
(25) Lewandowska, A.; Ołdziej, S.; Liwo, A.; Scheraga, H. A. *Proteins: Struct. Funct. Bioinf.* **2010**, *78*, 723–737.
(26) Lewandowska, A.; Ołdziej, S.; Liwo, A.; Scheraga, H. A. *Biopolymers* **2010**, *93*, 469–480.
(27) Makowska, J.; Bagińska, K.; Liwo, A.; Chmurzyński, L.; Scheraga, H. A. *Biopolymers: Peptide Science* **2008**, *90*, 724–732.
(28) Makowska, J.; Bagińska, K.; Skwierawska, A.; Liwo, A.; Chmurzyński, L.; Scheraga, H. A. *Biopolymers: Peptide Science* **2008**, *90*, 772–782.
(29) Ngyuyen, H.; Jager, M.; Moretto, A.; Gruebele, M.; Kelley, J. W. *Proc. Natl. Acad. Sci. U. S. A.* **2003**, *100*, 3948–3953.
(30) Sharpe, T.; Jonsson, A.; Rutheford, T. J.; Daggett, V.; Fersht, A. R. *Protein Sci.* **2007**, *16*, 2233–2239.
(31) Macias, M. J.; Gervais, V.; Civera, C.; Oschnikat, H. *Nat. Struct. Biol.* **2000**, *7*, 375–379.
(32) Vorobjev, Y. N.; Scheraga, H. A.; Hitz, B.; Honig, B. *J. Phys. Chem.* **1994**, *98*, 10940–10948.
(33) Vorobjev, Y. N.; Scheraga, H. A.; Honig, B. *J. Phys. Chem.* **1995**, *99*, 7180–7187.
(34) Ripoll, D. R.; Vorobjev, Y. N.; Liwo, A.; Vila, J. A.; Scheraga, H. A. *J. Mol. Biol.* **1996**, *264*, 770–783.
(35) Makowska, J.; Bagińska, K.; Makowski, M.; Jagielska, A.; Liwo, A.; Kasprzykowski, F.; Chmurzyński, L.; Scheraga, H. A. *J. Phys. Chem. B* **2006**, *110*, 4451–4458.
(36) Makowska., J.; Rodziewicz-Motowidło, S.; Bagińska, K.; Vila, J.; Liwo, A.; Chmurzyński, L.; Scheraga, H. A. *Proc. Natl. Acad. Sci. U. S. A.* **2006**, *103*, 1744–1749.
(37) Zagrovic, B.; Lipfert, J.; Sorin, E.; Millett, I. S.; van Gunsteren, W. F.; Doniach, S.; Pande, V. S. *Proc. Natl. Acad. Sci. U. S. A.* **2005**, 11698–11703.
(38) Plotnikov, V.; Rochalski, A.; Brandts, M.; Brandts, J. F.; Williston, S.; Frasca, V.; Lin, L. N. *Assay Drug Dev. Technol.* **2002**, *1*, 83–90.
(39) Bjerrum, N.; Unmack, A. *Kgl danskeVidenskab Selskab mat-fys Medd* **1929**, 9, 1, 126, 132, 141.
(40) Kugelmass, I. N. *Biochem. J.* **1929**, *23*, 587.
(41) Nims, L. F. *J. Am. Chem. Soc.* **1934**, *56*, 1110.
(42) Bates, R. G. *J. Res. Natl. Bur. Stand.* **1951**, *47*, 127.
(43) Bates, R. G.; Acree, S. F. *J. Res. Natl. Bur. Stand.* **1943**, *30*, 129.
(44) Kostrowicki, J.; Liwo, A. *Comput. Chem.* **1987**, *11*, 195–210.
(45) Kostrowicki, J.; Liwo, A. *Talanta* **1990**, *37*, 645–650.
(46) Ufnalski, W.; *Równowagi jonowe*; Wydawnictwa Naukowo-Techniczne: Warszawa, 2004; p 57.
(47) Rodante, F.; Fantauzzi, F.; Catalani, G. *Thermochim. Acta* **1998**, *311*, 43–49.
(48) Hamborg, E. S.; Versteeg, G. F. *J. Chem. Eng. Data* **2009**, *54*, 1318–1328.
(49) Shoghi, E.; Romero, L.; Reta, M.; Rafols, C.; Bosch, E. *J. Pharm. Biomed. Anal.* **2009**, *49*, 923–930.
(50) Rodante, F.; Vecchio, S.; Fantauzzi, F. J. *Thermal. Anal. Calorim.* **2001**, *66*, 79–90.
(51) Miyazawa, T. In *Poly-a-Amino Acids. Protein Models for Conformational Studies*; Fasman, G. D., Ed.; Marcel Dekker: New York, 1967; pp 69−103.